LASER ENGINEERED DISSOLVING MICRONEEDLES FOR ACTIVE TRANSDERMAL DELIVERY OF NADROPARIN CALCIUM

Yasmine A. Gomaa[a,c], **Martin J. Garland**[b], **Fiona McInnes**[a,1], **Labiba K. El-Khordagui**[c], **Clive Wilson**[a], and **Ryan F. Donnelly**[b,*]

[a]Strathclyde institute of pharmacy and biomedical sciences (SIPBS), University of Strathclyde, 161 Cathedral Street, Glasgow, G4 0RE Scotland, UK.

[b]School of Pharmacy, Queen's University of Belfast, 97 Lisburn Road, Belfast, BT9 7BL, Northern Ireland, UK.

[c]Department of Pharmaceutics, Faculty of Pharmacy, Alexandria University, El-Khartoum square, Alexandria, 21521, Egypt.

Abstract

There is an urgent need to replace the injection currently used for low molecular weight heparin (LMWH) multi-dose therapy with a non-invasive delivery device. In this study, laser-engineered dissolving microneedle (DMN) arrays fabricated from aqueous blends of 15% w/w poly (methylvinylether co maleic anhydride) have been fabricated as a potential device for the active transdermal delivery of nadroparin calcium (NC) as a model LMWH. An array loading of 630 IU of NC was achieved without compromising the array mechanical strength or the drug bioactivity. Application of NC-DMNs to dermatomed human skin (DHS) using the single step "poke and release" approach allowed permeation of approximately 10.6 % of the total NC load over a 48 h-study period. The cumulative amount of NC that permeated DHS at 24 h and 48 h attained 12.28 ± 4.23 IU/cm^2 and 164.84 ± 8.47 IU/cm^2, respectively. Skin permeation of NC could be modulated by controlling the DMN array variables, such as MN length and array density as well as application force to meet various clinical requirements including adjustment for body mass and renal function. NC-loaded DMN offer potentials as a relatively low cost functional delivery system for the transdermal delivery of LMWH and other macromolecules.

Keywords

low molecular weight heparin; nadroparin calcium; dissolving microneedles; anti-factor Xa activity; transdermal permeation

[*]Corresponding author: Ryan F. Donnelly School of Pharmacy, Queen's University of Belfast, 97 Lisburn Road, Belfast, BT9 7BL, Northern Ireland, UK. r.donnelly@qub.ac.uk Tel: +44 (0) 28 90 972 251, Fax: +44 (0) 28 90 247 794 .
[1]Drug Delivery International, Bio-Imaging Centre, Basement Medical Block, Within Glasgow Royal Infirmary, 84 Castle Street, Glasgow G4 0SF, UK.
Email addresses of authors: Yasmine Gomaa: yasmine87ag@yahoo.com ; Martin Garland: mgarland01@queens-belfast.ac.uk ; Fiona McInnes: f.mcinnes@dd-int.com ; Labiba El-Khordagui: lakhalil@alexpharmacy.edu.eg ; Clive Wilson: c.g.wilson@strath.ac.uk

1. Introduction

Low molecular weight heparins (LMWHs) are the most commonly used anticoagulants in the prophylaxis and treatment of deep vein thrombosis (DVT) [1] and pulmonary embolism [2]. Heparins are glycosaminoglycan macromolecules, whereas LMWHs are produced by chemical or enzymatic hydrolytic cleavage of unfractionated heparin (UFH) with an average molecular weight (MW) of 3-9 kDa [3]. LMWHs act by forming a complex with antithrombin III (AT III), resulting in the inactivation of a number of coagulation enzymesessentially responsible for fibrin clot formation [4]. Compared to UFH, LMWHs have a longer half-life, higher bioavailability, improved predictability of the pharmacodynamic effect, lower risk of heparin-induced thrombocytopenia and less binding to non-anticoagulant-related plasma proteins and platelets after injection [4-7]. Unfortunately, the physicochemical properties of LMWH, particularly high hydrophilicity, large MW and highly negative charge preclude their passive diffusion across biological barriers, resulting in poor systemic absorption which previously restricted their administration to the parenteral route [8]. This route is known to be associated with pain, inconvenience, potential risk of bleeding and the requirement of close monitoring in some cases [9]. In the four year period between 2005 and 2009, the National Patient Safety Agency reported 2716 safety incidents relating to dosing errors concerning LMWHs [10].

Several attempts have been made to enhance the bioavailability of LMWH through the oral [11], rectal [12], nasal [13, 14] and pulmonary routes [15, 16], though with limited success. Transdermal drug delivery presents an attractive alternative route for LMWH administration. However, research has been hampered by poor skin absorption of LMWH because of its unfavourable physicochemical properties and interaction with the *stratum corneum* (*SC*) [17]. Chemical, physical and carrier-mediated strategies have been adopted to overcome the *SC* barrier and permeabilize the skin to LMWH. These include the use of chemical skin penetration enhancers [18], ultrasound [9, 19], iontophoresis [17, 20], and liposomal transdermal delivery [21, 22], each of which has various degrees of success and drawbacks due to complexity making their commercialization rather difficult.

In recent years, microneedles (MN) arrays have emerged as an attractive physical technology to enhance skin permeability by breaching the *SC* in a painless and minimally-invasive manner. MNs create microchannels that permit enhanced skin permeation of small drug molecules, macromolecules and nanoparticles [23]. MNs are micron-sized structures, ranging from 50 to 1000 μm in length and about 300 μm diameter, usually projecting out from a patch-like support. The different types of MNs, their shapes, composition, fabrication methods, biomedical applications and safety have been reviewed [24, 25]. Two main approaches are adopted to deliver permeants into the skin using MN arrays. A two-step approach involves skin microporation with plain MNs followed by application of the drug formulation or patch (poke and patch). The second approach is a single-step administration combining skin microporation and drug delivery, based on the in-skin release of a drug coated on MN (coat and poke), loaded into dissolving microneedles (DMN) (poke and release) or a drug solution filled in hollow MNs (poke and flow)[26]. Apart from the simplicity of the single step DMN approach, they offer the advantage of no sharps left after removal. They are hence, self-dissolving and require no specified disposal procedures.

Previous attempts to enhance the transdermal delivery of LMWH using MN technology involved the use of the two-step "poke and patch" approach [17] or a LMWH-loaded single DMN inserted percutaneously [27]. However, the main limitations of these studies were the multistep-procedure adopted and wound formation, respectively. The aim of the present study was to enhance the transdermal delivery of a LMWH, nadroparin calcium (NC), using DMNs to achieve one-step administration of potential clinical applicability. The effect of DMN patch variables, such as NC loading, MN length and MN array density on the *in vitro* NC release from DMN patch and permeation through dermatomed human skin (DHS) was investigated to generate data to meet different NC dosage regimens.

2. Materials and methods

2.1. Materials

LMWH (Nadroparin Calcium (NC), MW: 4300 Da, anti-factor Xa activity: 105 IU/mg) was a gift from Glaxosmithkline (Glaxo Welcome Production, Notre Dame de Bondeville, France). HemosIL^{TM} Liquid Heparin assay kit was obtained from Instrumentation Laboratory (Lexington, USA). Gantrez® AN-139, a copolymer of methylvinylether co maleic anhydride (PMVE/MA), was provided by ISP Co. 120 Ltd. (Guildford, UK). Silastic® 9280/60E silicone elastomer was purchased from Dow Corning (Midland, MI, USA). 'Silver dag' - a colloidal silver - was purchased from Polysciences Inc. (Eppelheim, Germany). Phosphate buffer saline (PBS) tablets (pH 7.4) and trypan blue dye were purchased from Sigma-Aldrich (St. Louis, MO, USA).

2.2. Fabrication of dissolving microneedle (DMN) arrays

DMN arrays were fabricated using PMVE/MA copolymer and laser-engineered silicone micro-moulding, as described previously [28, 29]. Briefly, micro-moulds templates were fabricated by pouring silicone elastomer into an aluminium mould and cured overnight at 40°C. A laser beam (Coherent Avia, Coherent Inc., Pittsburgh, USA) with a wavelength of 355 nm and a pulse length of 30 ns (variable from 1 to 100 kHz) produced by a laser micromachining system (BluLase® Micromachining System, Blueacre Technology, Dundalk, Ireland) was used to produce MN moulds with different configurations. A 15% w/w aqueous solution of PMVE/MA was prepared by dispersing the required amount of the copolymer in ice-cold deionised water, followed by vigorous stirring and heating at 95.0°C until a clear gel of the acid hydrolysis product of the anhydride PMVE/MA was formed. The concentration of the polymer blend solution was readjusted to 15% with deionised water. The solution was poured into the silicone micro-moulds, centrifuged for 15 min at 3500 rpm and allowed to dry under ambient conditions for 24 h. DMN arrays with a base plate were removed from the micro-moulds. For the preparation of drug-loaded DMNs, a specific mass of NC was added to the % 15 w/w PMVE/MA aqueous solution prior to fabrication of the MN arrays. NC was loaded into both the needle shafts and the backing membrane (base plate). NC-DMN arrays of various drug loading (315, 630 or 945 IU/MN array), DMN length (400, 600 or 1000 μm) and array density (121, 196 or 361 MN/array) were fabricated. These are described in Table 1.

2.3. Imaging of the fabricated NC DMN arrays

The fabricated MN arrays were viewed by scanning electron microscopy (SEM). The arrays were mounted on aluminium stubs using double-sided adhesive tape and 'silver dag'. A SC515 SEM sputter coater (Polaron, East Grinstead, UK) was used to coat the arrays with a 20 nm-thick layer of gold / palladium. The arrays were observed under a JSM 6400 digital SEM (JEOL Ltd, Tokyo, Japan) and photomicrographs of MN structures were acquired. NCDMN arrays were also visually inspected for any defective morphology or NC precipitation and imaged using a digital camera.

2.4. Measurement of DMN mechanical strength upon NC loading

The effect of NC initial loading on the mechanical strength of NC-DMNs was assessed by measuring the percentage reduction in MN height after application of a known axial compression load (i.e., force applied parallel to the MN vertical axis) using a TA.XT-plus Texture Analyser (Stable Micro Systems, Surrey, UK) as reported previously [29]. In brief, DMN arrays were visualized using a light microscope (GXMGE-5 USB Digital Microscope, Laboratory Analysis Ltd., Devon, UK) to determine the initial height of DMN with the aid of the ruler function of the microscope software. DMN arrays were then attached to the moveable cylindrical probe of the Texture Analyser using double-sided adhesive tape. DMN arrays were pressed by the test station against a flat block of aluminium at a rate 0.5 mm/s for 30 s and a force of 0.36 N per MN pressed. Pre-test and post-test speeds were set at 1 mm/s and the trigger force was set at 0.049 N. This was followed by measuring the final height of each needle microscopically and calculation of the % reduction in DMN height. Data presented are the average of 5 measurements.

2.5. *In vitro* release from DMNs and effect of DMN variables

The *in vitro* drug release was determined by placing NC-DMN arrays with different loading, MN length and array density in 10-mL screw cap glass vials containing 5.3 mL PBS (pH 7.4) as a release medium. Sink conditions were maintained based on NC equilibrium solubility (10765 ± 275 IU/mL) determined at 37°C in the release medium. Vials were oscillated in a thermostatically controlled water bath (DMS360, Fischer Scientific, Leicestershire, UK) at 37°C at 200 oscillations /min. Samples, 200 μL each were withdrawn at 1, 2, 3, 4, 5, 10, 20, 30, 45 and 60 min. Released NC was determined using a biological assay based on NC biological activity (antifactor Xa activity). The amount of NC released after complete dissolution of the arrays was used to calculate the actual content. The percentage incorporation efficiency (% I.E.), calculated by dividing the actual amount of NC in DMN arrays by the theoretical NC loading, was used to assess NC biological activity following the micro-moulding process.

2.6. Biological analysis of NC

The biological activity of NC samples was determined by measuring the antifactor Xa activity using an automatic analyser (ACL [TM], Instrumentation Laboratory, Lexington, USA) and a biological assay kit. Briefly, a 50 μL aliquot of NC standard solution or sample was automatically mixed with 50 μL of AT III solution and incubated for 90 s at 37 °C to form a NC-AT complex. The mixture was then mixed with an excess of factor Xa (100 μL)

and incubated for 30 s at 37 °C. A fraction of factor Xa was neutralized by the [NC-AT] complex in proportion to the amount of NC. A 50 μL-aliquot of chromogenic peptide factor Xa substrate (S-2765 (N-α -Z-D-Arg-Gly-Arg-pNA.2 HCl) was added and the mixture incubated at 37 °C. The un-neutralized factor Xa catalyzes the splitting off of an orange dye (paranitroaniline) from the chromogenic peptide substrate. The absorbance of the dye measured at 405 nm every 2 s for 10 to 30 s of incubation was inversely proportional to the NC level in the sample. PBS was included as blank to determine the maximum absorbance value at zero NC concentration. Unknown concentrations of NC were determined from the obtained relationship between absorbance/min and the concentration of NC in the range of 0 to 0.8 IU/mL.

2.7. *In vitro* NC permeation studies and effect of DMN variables

Since a tissue thickness of about 200-400 μm represents the effective barrier to the MN-mediated skin penetration of drugs [30], two skin models were investigated. Full thickness porcine skin (~1200 μm) was selected to model the resistance of full thickness skin to MN penetration whereas DHS (~330 μm) was chosen to mimic the approximate distance between the skin surface and the dermis. Full-thickness cadaveric human skin samples were purchased from the National Disease Research Interchange (Philadelphia, PA). Samples were derived from the abdominal regions of elderly Caucasian females. Ethical and regulatory approval was granted for use of human skin samples and for subsequent experimentation. The skins were sectioned using a locally designed electric dermatome to produce 330 μm-thick samples. Full thickness porcine skin was obtained from ears of pigs (Landrace species), harvested immediately following slaughter at a local abattoir (Glasgow, UK). Skin was neither steam-sterilized nor boiled before use. The ears were sectioned using a scalpel to yield whole skin samples. Full-thickness skin was cut into circular samples with a surface area of ~4 cm^2, and the average thickness of skin samples, as measured by a digital micrometer, was 1164 ± 103 μm (n = 46). Both types of skin samples were wrapped in aluminium foil and stored at −80 °C for no longer than 6 months. The skins were allowed to thaw to room temperature for 1 h before use.

Prior to NC permeation experiments, skin samples were initially left in the Franz diffusion cells (PermeGear, Bethlehem, PA, USA), with their dermal side facing the receiver compartment, for 1 h to allow skin hydration. The skin was fixed to the rims of the receiver compartment using cynoacrylate adhesive (Super glue, WHSmith, UK). DMNs were applied to skin samples either manually or using a locally designed prototype simple spring-loaded piston with a one-button release applicator at output forces of 4, 7 and 11 N/MN array adjusted by using different spring settings (Springmasters Ltd., Redditch, UK) (Table 2). DMNs were kept in place during the experiment by application of a weight (8.25 gm) and by covering their upper surface with BluTack® (Bostik Ltd., Leicester, UK). The receiver cells contained 5.3 mL PBS, pH 7.4, which was stirred at 600 rpm and maintained at 37 ± 0.5 °C using a thermostatically-controlled water pump (Haake DC10, Karlsruhe, Germany). Samples (200 μL) were removed from the sampling arm at specific time intervals over 48 h. Each sample was replaced with an equal volume of fresh PBS adjusted to 37°C. Samples were analyzed for permeated NC using the biological assay method.

The procedure was also used to study the effect of DMN array variables, including NC loading (315 or 630 IU/ array of 600 μm needle length and of 121 MN/array density), DMN length (400, 600 and 1000 of 630 IU of NC/ array and of 121 MN/array density), array density (121, 196 and 361 MN/array of 630 IU of NC/ array and 600 μm needle length), and application force (4, 7 and 11 N/array applied to a 630 IU of NC/ array, 600 μm needle length and of 121 MN/array density) in single factor experiments on the permeation of NC through DHS. A solution of NC (630 IU/0.5 mL) in PBS, pH 7.4 was used as control on both untreated skin and DMN-treated skin (porcine and DHS). In this particular experiment, plain DMN arrays (600 μm, 121 MN/array) were inserted into the skin sample and retracted before application of the NC solution. Similar arrays, without the application of the NC solution, were used to test the interference of PMVE/MA copolymer that might pass to the receiver solution after MN dissolution with the biological assay of NC.

2.8. Trypan blue staining of MN-treated skin samples

The *SC* side of MN-treated DHS was covered with 0.4% w/v trypan blue dye in PBS (pH 7.4) in order to stain the microconduits created by DMN applied either manually or using the applicator at different output forces (4, 7, and 11 N/array). After 1 h, the dye was washed off under a flow of cold water. The *SC* side of each skin sample was examined and representative skin sites were photographed using a DFC320 camera (Leica Microsystems Wetzlar GmbH, Germany) attached to a DM LB2 light microscope (Leica Microsystems Wetzlar GmbH, Germany).

2.9. Statistical analysis

In vitro skin permeation data were analyzed by performing Student's unpaired t-test using Minitab 16 statistical software (Minitab Inc., State College, PA, USA) where $P < 0.05$ was considered statistically significant.

3. Results

3.1. Imaging of fabricated NC DMN arrays

Fig. 1 shows the NC-DMN arrays fabricated in the study, showing different MN lengths and densities. Fig. 1(f) is a photo image of NC-DMN indicating no sign of NC precipitation.

3.2. Measurement of DMN mechanical strength upon NC loading

The effect of NC loading (1, 2 and 3% corresponding to 315, 630 and 945 IU/array respectively) on the mechanical strength of DMN arrays was assessed using a force of 0.36 N/needle and % reduction in MN height as parameter. Plain MN arrays showed a 15.37 ± 0.78 % height reduction upon application of a force of 0.36 N/needle. Loading DMN with NC resulted in a greater % height reduction, the effect being NC loading dependent (16.94 ± 0.82, 18.03 ± 0.55 and 20.21 ± 0.89 at 1, 2 and 3% NC loading respectively). The difference between % height reduction of plain and all NC-loaded DMN was statistically significant ($P < 0.05$). Whilst the difference between % height reduction by 1% and 2% loading did not reach significance ($P = 0.05$), the difference between the effect of 2% and 3% NC loading was statistically significant ($P = 0.003$). Accordingly, DMN arrays with 3% NC loading

were excluded from further experiments as it was predicted that their lower mechanical strength would result in poor skin penetration.

3.3. Biological analysis of NC

NC was determined using an antifactor Xa activity-based biological assay, highly sensitive to the pentasaccharide sequence unique to heparin, heparan sulphate and LMWH [31]. A linear NC concentration-bioactivity relationship was obtained over the concentration range 0-0.8 IU/mL (R^2 = 0.9863). The actual NC content of DMN arrays of theoretical content 315 and 630 IU was 295.24 ± 40.46 and 561.23 ± 23.48 IU/array, respectively. This is approximately equivalent to a % I.E. of 94 and 89%, respectively.

3.4. *In vitro* release of NC from DMN arrays and effect of DMN variables

Data for *in vitro* release of NC from DMN arrays with different drug loading, MN length and MN densities are shown in Fig. 2-4. Increasing NC loading (315 *vs* 630 IU/array) resulted in increased initial NC release (Fig. 2). The % release at 5 min was 49 % and 67% for arrays containing 315 and 630 IU/array, respectively. Almost complete release of NC was achieved in 60 min in both cases. Increasing MN length also resulted in a corresponding increase in initial NC release (Fig. 3). Release at 5 min attained 56, 67 and 100% from 400, 600 and 1000 μm DMN, respectively. Complete NC release from 400 and 600 μm arrays was achieved in 60 min. Further, denser DMN arrays were associated with enhanced drug release both in terms of release rate and extent (Fig. 4). The % release at 5 min was 67, 84 and 96% for DMN arrays with 121, 196 and 361 MN/array, respectively.

3.5. *In vitro* NC permeation studies and effect of DMN variables

The influence of skin model, MN variables (loading, length and density) and mode of application of DMN arrays on the *in vitro* skin permeation of NC were investigated.

3.5.1. Influence of skin model—Two skin models, full thickness porcine skin (~1200 μm) and DHS (~330 μm) were tested using DMN arrays (600 μm MN length and 121 MN/array density) containing 630 IU/array NC load. An applicator was used to insert the arrays at an output force of 11 N/array. Application of (630 IU/0.5 mL) NC control solution expectedly didn't result in skin permeation for up to 48 hr through porcine and DHS. Skin pretreatment with plain DMN arrays didn't improve permeation of NC from solution in both skin models. Further, dissolved PMVE/MA polymer did not interfere with the biological assay of NC.

Permeation data obtained following skin treatment with NC-DMN arrays showed minimal permeation of NC through full thickness porcine skin (Fig. 5). A cumulative amount of 1.69 ± 0.21 IU /cm² was delivered at 48 h accounting for less than 1% of the actual NC load/ array. However, the cumulative amount of NC permeating DHS was statistically larger (*P* < 0.005) throughout the study with a cumulative amount of 103.31 ± 12.54 IU /cm² corresponding to 6.63 ± 0.80% of the actual NC load/ array permeating the skin at 48 h. Accordingly, full thickness porcine skin was not used in subsequent experiments.

3.5.2. Influence of NC loading in DMN arrays—Manual treatment of DHS skin with NC-DMN arrays of 315 and 630 IU of NC/ array resulted in more or less similar permeation profiles (Fig. 6). Although the mean cumulative amount of NC permeating DHS at 48 h for the 630 IU/array (53.15 ± 7.05 IU /cm^2) was less than that for the 315 IU/array (65.95 ± 6.25 IU /cm^2), the difference did not reach statistical significance ($P = 0.067$).

3.5.3. Influence of NC DMN length—The influence of MN length was investigated using NC-DMN arrays (630 IU/array, 121 MN/array) with 400, 600 and 1000 μm needle length. Results showed a marked effect of MN length on NC delivery (Fig. 7). In particular, increasing the needle length from 400 to 600 μm led to a significant increase in cumulative amount permeating from 3.25 ± 1.17 IU/cm^2 to 9.23 ± 0.77 IU /cm^2 at 24 h and from 5.36 ± 1.89 IU /cm^2 to 53.15 ± 7.05 IU /cm^2 at 48 h ($P< 0.01$ each). Further increase in length to 1000 μm resulted in a much greater enhancement in NC permeation at 24 h (150.81 ± 7.45 IU /cm^2) and 48 h (158.63 ± 9.75 IU /cm^2) compared to both MN arrays of 400 and 600 μm in length ($P= 0.001$ each). This corresponded to a 10.18 ± 0.63 % permeation of the NC load at 48 h.

3.5.4. Influence of NC DMN density—The influence of needle density (121, 196 and 361 MN/arrays) of DMN arrays with 630 IU of NC/array and 600 μm long DMN on NC permeation is shown in Fig. 8. DMN array density did not significantly affect NC permeation for up to 24 hr. However at 48 hr, increasing needle density from 121 to 196 MN/array resulted in a significant increase in cumulative permeation from 53.15 ± 7.05 IU /cm^2 to 64.85 ± 9.31 IU /cm^2 ($P = 0.029$). Application of the densest 361 MN/arrays led to a much larger increase in cumulative NC permeation ($P <0.00005$) reaching 164.84 ± 8.47 IU /cm^2 which corresponds to 10.57 ± 0.54% of the NC load/array.

3.5.5. Influence of MN application force—An applicator was used to insert DMN arrays (630 IU NC/array, 600 μm long and 121 MN/array dense) into DHS. Springs were selected to provide output forces of 4, 7 and 11 N/array. Fig. 9 shows the influence of increasing application force on NC permeation. Data obtained with manual application were included for comparison. NC permeation increased as a function of the applicator force. Insertion of the MN arrays at an application force of 11N/array resulted in a cumulative NC permeation of 75.41 ± 11.91 IU /cm^2 at 24 h and 103.31 ± 12.54 IU /cm^2 at 48 hr that was significantly ($P <0.05$) larger than that achieved by all tested application forces. On the other hand, manual application resulted in the lowest NC permeation throughout the study.

3.6. Trypan blue staining of MN-treated skin samples

The effect of mechanical application at different applicator output forces in comparison to manual application on skin microporation with DMN was visualized with trypan blue staining (Fig. 10). Blue spots were evident on *SC* at all tested MN application forces and manual mode indicating successful penetration of generally all DMN of the array. Importantly, the intensity and/or width of the observed spots varied according to the mode of MN application. Manual application resulted in blue spots of varying width, indicating unequal insertion of all needles of the array. However, using the applicator, the spots' width was apparently consistent and their intensity increased roughly with the increase in applied

force. Few spots of low intensity were evident on skin samples into which MN arrays were inserted at an application force of 4 N. The greatest intensity was obtained following MN application at a force of 11 N. Staining results were more or less consistent with permeation data.

4. Discussion

The objective of this study was to assess DMNs arrays as a potential carrier for the active transdermal delivery of macromolecular therapeutics using NC as a model macromolecule. NC selection was justified by its clinical importance in the prophylaxis and treatment of DVT and pulmonary embolism and the urge to replace the strategy currently used for LMWH multidose therapy with a minimally-invasive delivery route. Attempts to deliver LMWH across the skin using different enhancement strategies have been challenged by hydrophilicity, high MW, negative charge and interaction of LMWH with the *SC* [32]. MN, a functional skin delivery system offers great promise for transdermal delivery of drugs and macromolecules lacking optimal physicochemical properties for skin permeation [33]. In previous attempts to enhance transdermal delivery of LMWH using MN technology, either a single DMN loaded with LMWH having a mean length of 1.52 mm and basal diameter of 0.51 mm was inserted percutaneously in rats [27] or arrays of 28 maltose DMN of 500 μm in length were used to perturb excised rat skin followed by the application of LMWH according to the two-step "poke and patch" approach [17]. However, DMN arrays with greater MN plurality, LMWH dose distributed between MN projections and base plate to modulate permeation profile and applied using the single step "poke and release" approach to avoid *SC*-LMWH interaction may overcome limitations of previous attempts and provide for greater clinical applicability. This was the subject of the present study. DMN arrays were fabricated using aqueous blends of 15% w/w of an inexpensive polymer (PMVE/MA) and a mild micro-moulding process that did not involve harsh conditions in order to preserve NC bioactivity. Incorporating NC in the needle shafts only would limit the NC dose to less than 1 mg in order to maintain adequate mechanical strength. Therefore, NC was incorporated in both the needle shafts and the base plate, which allowed delivery of both a bolus and maintenance NC dose, respectively. Maintenance of NC bioactivity following the micro-moulding process was confirmed by determining % I.E. based on anti-Xa activity of NC after complete drug release from DMN. A relatively high % I.E. was obtained (~ 94 and 89 % for DMN with 1 and 2% drug loading respectively).

The amount of NC loaded into DMN was selected taking into consideration the adverse effect of excessive drug loading on the mechanical strength of the DMN arrays. Based on measurements of % MN height reduction upon application of an axial compression force, drug loading up to 2% was deemed acceptable. Arrays with 315 (1%) and 630 IU (2%) of NC loading resisted compressive forces with only 16.9 and 18% reduction in height respectively. Indeed, incorporation of a water soluble drug such as NC is expected to soften the Gantrez® AN-139 MN polymer upon moulding, which may result in failure of MN insertion into the skin. This has been reported for MN arrays composed of 20% w/w Gantrez® AN-139 loaded with >1% theophylline [34] and PLGA arrays loaded with 10% calcein [35].

In vitro release experiments were conducted to investigate the effect of MN variables, namely drug loading, MN length and array density on the release of NC. Drug release was generally fast with $t_{50\%}$ (time required for 50% release) less than 5 min in many instances. This is a consequence of the high solubility of both the polymeric MN material and NC in PBS (pH 7.4). MN variables only affected initial release rate. Data revealed faster NC release using arrays with higher drug content (630 > 315 IU/array), longer needles (1000>600>400 μm) and denser plurality (361>196>121 MN/array). Increasing MN length and array density expectedly increase the surface area of MN exposed to the release medium. However, the fast drug release observed *in vitro* may not be extended to *in vitro* permeation experiments due to difference between the volumes of the two release media employed. It has been demonstrated that dissolution of DMN arrays starts within a few minutes after insertion into the skin [36]. The needle shafts dissolve in the interstitial fluids, releasing the drug entrapped in the needle shafts (bolus dose), while the MN base plate serves as a controlled release drug reservoir. In particular, drug in the base plate is delivered by a combination of polymer swelling as a result of imbibition of interstitial fluid drawn out of the skin resulting in adhesion to skin surface as confirmed by optical coherence tomography (OCT) *in vivo* (unpublished data). This is followed by molecular diffusion into the skin *via* channels created by MN treatment enabling sustained drug delivery. This was further confirmed by the swelling and softening of the base plate after 48 h.

In vitro skin permeation experiments may be conducted using different types of skin models. In a preliminary study, full thickness porcine skin (1200 μm), as a readily available and inexpensive skin model, and DHS (330 μm) were used for NC permeation. A control solution of NC expectedly failed to permeate both skin models up to 48 h, because of the physicochemical properties of the drug. This also confirmed the integrity of the skin samples used. A similar observation was reported for permeation of heparin through human skin *in vitro* [37]. This can be explained partially by the high MW, high negative surface charge and hydrophilicity, rendering NC a bad candidate for passive diffusion through the skin. It has been suggested that NC, being negatively charged, would be subjected to repulsive forces generated by the skin's net negative charge [21]. Moreover, several *in vitro* studies have suggested an interaction of LMWH with the *SC,* which could further explain the observed lack of permeation through intact skin. An *in vitro* study showed the preferential interaction and binding of LMWH to keratinocytes abundant in the *SC* [38]. Such interaction was mediated through the GlcNAc6S moiety on the LMWH polysaccharide chain [39]. Another study demonstrated similar interactions using differential scanning calorimetry and Fourier transform infrared spectroscopy studies [17]. In view of this, *in vitro* transdermal delivery of LMWH through tape-stripped excised rat skin was shown to be enhanced significantly (flux of 4.07 IU/cm^2/h) compared to either intact skin or skin pre-treated by iontophoresis (63-fold higher) or ultrasound (70-fold higher)[17]. Although tape stripping and removal of *SC* would provide an efficient means for enhancing the transdermal delivery of LMWH, it is not a recognized practical alternative.

Breaching the *SC* with NC-loaded DMN resulted in marked enhancement of NC transdermal delivery across DHS (a 61-fold increase in NC permeation at 48 h), while drug permeation through full thickness porcine skin remained minimal. Data for DHS indicated both

suitability of DHS for the *in vitro* modeling of skin permeation and effectiveness of DMN as a carrier for the active transdermal delivery of macromolecules. Indeed, full thickness skin presents a longer path length for drug transport, leading to permeation retardation. Moreover, dermatomed skin is better hydrated, a requirement for initiating dissolution of the DMN polymer matrix and drug release. It has been shown that 80% of theophylline incorporated in DMN arrays (900 μm MN length) permeated dermatomed neonatal porcine skin (350 μm) in 24 h, while only 20% permeation was observed for the same period when full thickness neonatal porcine skin (1200 μm) was used [40]. Based on data obtained in the present study and data reported earlier, DHS was used for further experiments.

The effect of selected variables on the performance of DMN as a functional carrier for transdermal delivery of macromolecules was demonstrated using DHS and arrays with different NC loading, MN length and array density. Despite fast *in vitro* NC release, permeation of NC through DHS generally showed a diffusion lag period extending over several hours. This was followed by NC permeation over the 48 h study period. Sustained delivery of NC can be attributed to the reservoir effect of the base plate [36]. Lag periods have been observed for sonophoresis-assisted transport of LMWH in rats [41] and for sulforhodamine incorporated in carboxymethycellulose DMN [36]. Drug permeation kinetics from DMN and the length of the lag period depend on the properties of the MN array matrix material [36].

Doubling NC loading while keeping other DMN array variables constant did not significantly change the amount of NC permeating DHS throughout the *in vitro* permeation study. The effect of drug loading on the skin permeation of drug incorporated in DMN has been controversial. While permeation of sulforhodamine loaded in carboxymethylcellulose MN arrays at a concentration of 30% w/w was~3 times greater than a similar system containing 10 % w/w when inserted in human cadaver epidermis [36], an insignificant decrease in the immunoglobulin G (IgG) flux through skin pre-treated with two-layered maltose MNs as a result of increasing concentration from 20 to 40 mg/mL was observed [42]. Decreased permeation at higher drug loading may be attributed to skin saturation relative to the donor solution beyond which the transport becomes independent of concentration [42].

NC permeation across DHS was enhanced by increasing MN length, array density and application force. Regarding the NC permeation-enhancing effect of longer DMN, a similar trend has been observed for the permeation of theophylline across both dermatomed and full thickness neonatal porcine skin [40] and IgG across human skin [42]. It is worth noting that, even though MN do not penetrate to their full length into the skin because of skin viscoelasticity and MN design [40, 43], DMN fully dissolve in the skin, probably due to transport of interstitial fluid from the skin up the needle shaft [36]. Given that the *SC* in human skin is about 10 to 20 μm thick, penetration of the 600 μm needle to 10-30% of its length (about 60-180 μm) should be sufficient for breaching the *SC* and delivering NC to deeper tissues [44]. Despite differences in the volume of release fluid, increasing the DMN length enhanced both *in vitro* NC release and NC permeation across DHS.

Similarly, an increase in density of the MN arrays was found to significantly increase skin permeation of NC with lack of "bed of nail" phenomenon, i.e. insufficient pressure per individual MN at higher density of solid MNs, reported for the "poke and patch" drug delivery approach [45]. According to this approach, the MN array is inserted in the skin and then removed to apply the drug formulation. MN retraction allows partial closure of the MN-created microconduits. However, DMN arrays are usually left in the skin with the aid of applied pressure, which allows pores to remain open by the gel formed upon dissolution of the DMN polymeric material. Thus, denser MN arrays might serve as a multiport delivery device for incorporated NC, enhancing its permeation. Such effects might offset the unequal pressure exerted on individual MNs. Results obtained in this study are consistent with those reported previously [46]. Further, OCT demonstrated that increasing array density did not affect penetration depth of DMN arrays with 600 μm long MN inserted into neonatal porcine skin [40].

Finally, using an applicator at increasing output forces (4, 7, and 11 N/array) caused a significant enhancement in NC permeation, compared to manual application, which was also associated with a longer lag period. Using the applicator even at the lowest application force (4 N/array), had a significantly ($P = 0.02$) marked effect on the NC delivery at 24 h compared to manual application. This can be attributed to deeper penetration of DMN at greater application force with the creation of wider pores. OCT studies on *in situ* dissolution of DMN arrays have shown dependence of penetration depth into neonatal porcine skin on the force of application [40]. A possible explanation could be the greater velocity by which the DMNs were inserted [47, 48] or the damage of tissue upon increasing the force of application, leading to deeper penetration [49]. In general, MN will only be able to penetrate the skin when the force of application exceeds the restrictive opposing force by the skin elasticity [50, 51]. Visualization of insertion sites with trypan blue staining indicated successful insertion of all MN of the array following manual or mechanical application, though the size of pores created mechanically was more consistent. Increasing mechanical application force led to the formation of wider and presumably deeper pores which might explain faster NC permeation. Hence for clinical application, it would be better to use an applicator at a definite output force to ensure effective performance and reduce variations.

Based on results obtained, DMN arrays proved successful to enhance the *in vitro* permeation of LMWH across DHS. Permeation could be modulated by controlling DMN variables and the force applied for inserting arrays into the skin. A cumulative permeation of about 165 IU/cm^2 (10.6% of NC loading) in 48 h could be achieved using DMN arrays with 630 IU of NC/array, 600 μm MN length and 361 MN/array density. This sustained anti-Xa activity should presumably improve antithrombotic therapy [41]. The total amount of NC permeating DHS at 48 h accounts for permeation of NC from both the needle shafts and the base plate since the NC in needles represents 5.8% only of the total load. Incomplete NC permeation during the 48 h-study period can be explained at least in part by possible retardation of NC diffusion from the base plate, due to blocking of the created MN-created microchannels by the slowly dissolving polymeric matrix, as reported previously in a similar study [52]. Moreover, possible interaction between NC released from DMNs and the epidermal and/or dermal cells in the surrounding tissues cannot be discounted [38].

The transdermal delivery of 150.81 ± 7.45 IU NC across 0.36 cm^2 in 24 h using DMN arrays of 630 IU of NC, 1000 μm long and 121 MNs can be considered therapeutically relevant. For instance, a patch of 6.5 cm^2 would deliver 2723 IU of NC in 24 h. This amount is comparable to a typical therapeutic dose generally given subcutaneously to an average weight human (70 kg) for prophylaxis of DVT and pulmonary embolism (41 IU/kg) and orthopaedic surgeries (38 IU/kg) [53]. This could be further tailored by increasing the area of the MN array patch to meet various dosage regimens required. For example, arrays of 14 cm^2 could be used to treat DVT (85 IU/kg) and unstable coronary artery diseases (86 IU/kg) [53].

5. Conclusions

In this study, economic DMN arrays fabricated under mild micro-moulding conditions are presented as a potential device for the active transdermal delivery of NC, a model macromolecular therapeutic with challenging resistance to passive skin absorption. The array could be loaded with up 630 IU of NC without compromising its mechanical strength or the drug bioactivity. NC could permeate DHS over a 48 h-study period. Apart from the known benefits of MN technology in the transdermal delivery of drugs with poor passive skin absorption, DMN arrays intended for simultaneous insertion and drug delivery proved particularly suitable for LMWH, known to interact with the *SC*. Direct extrapolation of data obtained to *in vivo* permeation of NC across full thickness human skin is, of course, not straight forward. However, DMN patches offer potential in delivering therapeutic doses of NC. This could be achieved by modulating drug release and increasing the area of the MN array patch to meet various in-use clinical requirements. Further *in vivo* studies are needed to demonstrate the activity of LMWH delivered by DMN arrays.

Acknowledgments

Glossary

MN	Microneedle
DMN	dissolving microneedle
NC	nadroparin calcium

References

[1]. Harrison L, McGinnis J, Crowther M, Ginsberg J, Hirsh J. Assessment of outpatient treatment of deep-vein thrombosis with low-molecular-weight heparin. Arch. Intern. Med. 1998; 158:2001–2003. [PubMed: 9778199]

[2]. Hyers TM, Agnelli G, Hull RD, Weg JG, Morris TA, Samama M, Tapson V. Antithrombotic therapy for venous thromboembolic disease. Chest. 1998; 114:561S–578S. [PubMed: 9822063]

[3]. Song YK, Kim CK. Topical delivery of low-molecular-weight heparin with surface-charged flexible liposomes. Biomaterials. 2006; 27:271–280. [PubMed: 16039711]

[4]. Hirsh J, Warkentin TE, Shaughnessy SG, Anand SS, Halperin JL, Raschke R, Granger C, Ohman EM, Dalen JE. Heparin and low-molecular-weight heparin: mechanisms of action, pharmacokinetics, dosing, monitoring, efficacy, and safety. Chest. 2001; 119:64S–94S. [PubMed: 11157643]

[5]. Carter CJ, Kelton JG, Hirsh J, Cerskus A, Santos AV, Gent M. The relationship between the hemorrhagic and antithrombotic properties of low molecular weight heparin in rabbits. Blood. 1982; 59:1239–1245. [PubMed: 7082826]

[6]. Frydman AM, Bara L, Le Roux Y, Woler M, Chauliac F, Samama MM. The antithrombotic activity and pharmacokinetics of enoxaparine, a low molecular weight heparin, in humans given single subcutaneous doses of 20 to 80 mg. J. Clin. Pharmacol. 1988; 28:609–618. [PubMed: 2851016]

[7]. Liautard C, Nunes AM, Vial T, Chatillon F, Guy C, Ollagnier M, Descotes J. Low-molecular-weight heparins and thrombocytosis. Ann. Pharmacother. 2002; 36:1351–1354. [PubMed: 12196050]

[8]. Frydman A. Low-molecular weight heparins: an overview of their pharmacodynamics, pharmacokinetics and metabolism in humans. Hemastatis. 1996; 26:24–38.

[9]. Mitragotri S, Kost J. Transdermal delivery of heparin and low-molecular weight heparin using low-frequency ultrasound. Pharm. Res. 2001; 18:1151–1156. [PubMed: 11587487]

[10]. National Patient Safety Agency. Reducing treatment dose errors with low molecular weight heparins. 2010 NPSA/2010/RRR014.

[11]. Motlekar NA, Youan BB. The quest for non-invasive delivery of bioactive macromolecules: a focus on heparins. J. Control. Release. 2006; 113:91–101. [PubMed: 16777255]

[12]. Nissan A, Ziv E, Kidron M, Bar-On H, Friedman G, Hyam E, Eldor A. Intestinal absorption of low molecular weight heparin in animals and human subjects. Haemostasis. 2000; 30:225–232. [PubMed: 11251329]

[13]. Arnold J, Ahsan F, Meezan E, Pillion DJ. Nasal administration of low molecular weight heparin. J. Pharm. Sci. 2002; 91:1707–1714. [PubMed: 12115833]

[14]. Mustafa F, Yang T, Khan MA, Ahsan F. Chain length-dependent effects of alkylmaltosides on nasal absorption of enoxaparin. J. Pharm. Sci. 2004; 93:675–683. [PubMed: 14762906]

[15]. Qi Y, Zhao G, Liu D, Shriver Z, Sundaram M, Sengupta S, Venkataraman G, Langer R, Sasisekharan R. Delivery of therapeutic levels of heparin and low-molecular-weight heparin through a pulmonary route. Proc. Natl. Acad. Sci. USA. 2004; 101:9867–9872. [PubMed: 15226520]

[16]. Yang T, Mustafa F, Bai S, Ahsan F. Pulmonary delivery of low molecular weight heparins. Pharm. Res. 2004; 21:2009–2016. [PubMed: 15587922]

[17]. Lanke SS, Kolli CS, Strom JG, Banga AK. Enhanced transdermal delivery of low molecular weight heparin by barrier perturbation. Int. J. Pharm. 2009; 365:26–33. [PubMed: 18801420]

[18]. Xiong GL, Quan D, Maibach HI. Effects of penetration enhancers on in vitro percutaneous absorption of low molecular weight heparin through human skin. J. Control. Release. 1996; 42:289–296.

[19]. Mitragotri S. Healing sound: the use of ultrasound in drug delivery and other therapeutic applications. Nat. Rev. Drug Discov. 2005; 4:255–260. [PubMed: 15738980]

[20]. Pacini S, Punzi T, Gulisano M, Cecchi F, Vannucchi S, Ruggiero M. Transdermal delivery of heparin using pulsed current iontophoresis. Pharm. Res. 2006; 23:114–120. [PubMed: 16362453]

[21]. Betz G, Nowbakht P, Imboden R, Imanidis G. Heparin penetration into and permeation through human skin from aqueous and liposomal formulations in vitro. Int. J. Pharm. 2001; 228:147–159. [PubMed: 11576777]

[22]. Song YK, Hyun SY, Kim HT, Kim CK, Oh JM. Transdermal delivery of low molecular weight heparin loaded in flexible liposomes with bioavailability enhancement: comparison with ethosomes. J. Microencapsul. 2011; 28:151–158. [PubMed: 21425940]

[23]. McAllister DV, Wang PM, Davis SP, Park JH, Canatella PJ, Allen MG, Prausnitz MR. Microfabricated needles for transdermal delivery of macromolecules and nanoparticles:

fabrication methods and transport studies. Proc. Natl. Acad. Sci. USA. 2003; 100:13755–13760. [PubMed: 14623977]

[24]. Prausnitz MR. Microneedles for transdermal drug delivery. Adv. Drug Deliv. Rev. 2004; 56:581–587. [PubMed: 15019747]

[25]. Donnelly RF, Singh T.R. Raj, Woolfson AD. Microneedle-based drug delivery systems: microfabrication, drug delivery, and safety. Drug Deliv. 2010; 17:187–207. [PubMed: 20297904]

[26]. Bariya SH, Gohel MC, Mehta TA, Sharma OP. Microneedles: an emerging transdermal drug delivery system. J. Pharm. Pharmacol. 2012; 64:11–29. [PubMed: 22150668]

[27]. Ito Y, Murakami A, Maeda T, Sugioka N, Takada K. Evaluation of self-dissolving needles containing low molecular weight heparin (LMWH) in rats. Int. J. Pharm. 2008; 349:124–129. [PubMed: 17826015]

[28]. Gomaa YA, Morrow DI, Garland MJ, Donnelly RF, El-Khordagui LK, Meidan VM. Effects of microneedle length, density, insertion time and multiple applications on human skin barrier function: assessments by transepidermal water loss. Toxicol. In Vitro. 2010; 24:1971–1978. [PubMed: 20732409]

[29]. Donnelly RF, Majithiya R, Singh TRR, Morrow DIJ, Garland MJ, Demir YK, Migalska k. Ryan E, Gillen D, Scott CJ, Woolfson AD. Design, optimization and characterization of polymeric microneedle arrays prepared by a novel laser-based micromoulding technique. Pharm. Res. 2011; 28:41–57. [PubMed: 20490627]

[30]. Scheuplein RJ. Mechanism of percutaneous absorption. II. Transient diffusion and the relative importance of various routes of skin penetration. J. Invest. Dermatol. 1967; 48:79–88. [PubMed: 6018244]

[31]. Mulloy B, Hogwood J, Gray E. Assays and reference materials for current and future applications of heparins. Biologicals. 2010; 38:459–466. [PubMed: 20338781]

[32]. Sznitowska M, Janicki S. Percutaneous absorption of heparin: a critical review of experimental results. Pol. Merkur. Lekarski. 2000; 7:58–63. [PubMed: 10765658]

[33]. Shah, VP. Transdermal drug delivery system regulatory issues. In: Guy, RH.; Hadgraft, J., editors. Transdermal Drug Delivery. Marcel Dekker Inc; New York: 2003. p. 361-367.

[34]. Donnelly RF, Majithiya R, Thakur RRS, Desmond DIJ, Garland MJ, Demir YK, Migalska K, Ryan E, Gillen D, Scott CJ, Woolfson AD. Design and physicochemical characterization of optimized polymeric microneedle arrays prepared by a novel laser-based micromoulding technique. Pharm. Res. 2011; 28:41–57. [PubMed: 20490627]

[35]. Park JH, Allen MG, Prausnitz MR. Polymer microneedles for controlled-release drug delivery. Pharm. Res. 2006; 23:1008–1019. [PubMed: 16715391]

[36]. Lee JW, Park JH, Prausnitz MR. Dissolving microneedles for transdermal drug delivery. Biomaterials. 2008; 29:2113–2124. [PubMed: 18261792]

[37]. Prausnitz MR, Edelman ER, Gimm JA, Langer R, Weaver JC. Transdermal delivery of heparin by skin electroporation. Nat. Biotechnol. 1995; 13:1205–1209.

[38]. Parisel C, Saffar L, Gattegno L, Andre V, Abdul-Malak N, Perrier E, Letourneur D. Interactions of heparin with human skin cells: binding, location, and transdermal penetration. J Biomed. Mater. Res. A. 2003; 67:517–523. [PubMed: 14566793]

[39]. Hozumi K, Suzuki N, Nielsen PK, Nomizu M, Yamada Y. Laminin alpha1 chain LG4 module promotes cell attachment through syndecans and cell spreading through integrin alpha2beta1. J. Biol. Chem. 2006; 281:32929–32940. [PubMed: 16945929]

[40]. Donnelly RF, Garland MJ, Morrow DIJ, Migalska K, Singh TRR, Majithiya R, Woolfson AD. Optical coherence tomography is a valuable tool in the study of the effects of microneedle geometry on skin penetration characteristics and in-skin dissolution. J. Control. Release. 2010; 147:333–341. [PubMed: 20727929]

[41]. Mitragotri S, Blankschtein D, Langer R. Transdermal drug delivery using low-frequency sonophoresis. Pharm. Res. 1996; 13:411–420. [PubMed: 8692734]

[42]. Li G, Badkar A, Nema S, Kolli CS, Banga AK. In vitro transdermal delivery of therapeutic antibodies using maltose microneedles. Int. J. Pharm. 2009; 368:109–115. [PubMed: 18996461]

[43]. Martanto W, Moore JS, Couse T, Prausnitz MR. Mechanism of fluid infusion during microneedle insertion and retraction. J. Control. Release. 2006; 112:357–361. [PubMed: 16626836]

[44]. Shirkhanzadeh M. Microneedles coated with porous calcium phosphate ceramics: effective vehicles for transdermal delivery of solid trehalose. J. Mater. Sci. Mater. Med. 2005; 16:37–45. [PubMed: 15754142]

[45]. Yan G, Warner KS, Zhang J, Sharma S, Gale BK. Evaluation needle length and density of microneedle arrays in the pretreatment of skin for transdermal drug delivery. Int. J. Pharm. 2010; 391:7–12. [PubMed: 20188808]

[46]. Garland MJ, Caffarel-Salvador E, Migalska K, Woolfson AD, Donnelly RF. Dissolving polymeric microneedle arrays for electrically assisted transdermal drug delivery. J. Control. Release. 2012; 159:52–59. [PubMed: 22265694]

[47]. Kendall MA, Chong YF, Cock A. The mechanical properties of the skin epidermis in relation to targeted gene and drug delivery. Biomaterials. 2007; 28:4968–4977. [PubMed: 17720240]

[48]. Crichton ML, Ansaldo A, Chen X, Prow TW, Fernando GJ, Kendall MA. The effect of strain rate on the precision of penetration of short densely-packed microprojection array patches coated with vaccine. Biomaterials. 2010; 31:4562–4572. [PubMed: 20226519]

[49]. Roxhed N, Gasser TC, Griss P, Holzapfel GA, Stemme G. Penetration-enhanced ultrasharp microneedles and prediction on skin interaction for efficient transdermal drug delivery. J. Microelectromech. Syst. 2007; 16:1429–1440.

[50]. Aoyagi S, Izumi H, Fukuda M. Biodegradable polymer needle with various tip angles and consideration on insertion mechanism of mosquito's proboscis. Sens. Act A. 2008; 143:20–28.

[51]. Kong X, Wu C. Measurement and prediction of insertion force for the mosquito fascicle penetrating into human skin. J. Bionic. Eng. 2009; 6:143–152.

[52]. Migalska K, Morrow DI, Garland MJ, Thakur R, Woolfson AD, Donnelly RF. Laser-engineered dissolving microneedle arrays for transdermal macromolecular drug delivery. Pharm. Res. 2011; 28:1919–1930. [PubMed: 21437789]

[53]. Lacy, CF.; Armstrong, LL.; Goldman, MP.; Lance, LL. Nadroparin. 14th ed. Lexi-Comp; Hudson, Ohio: 2006-2007. p. 1181-1182.
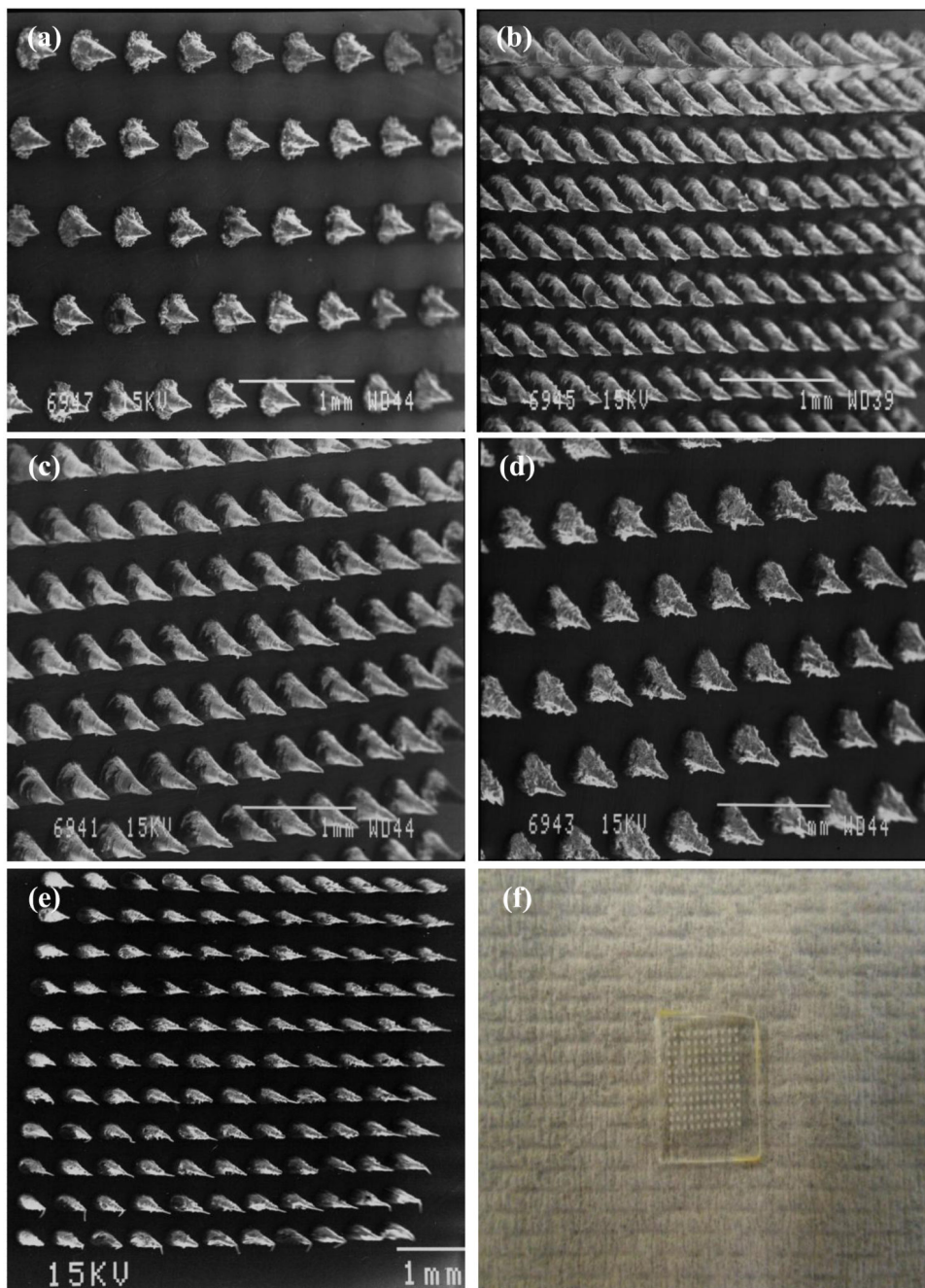
Figure 1. SEM images of laser engineered NC DMN arrays, (a) length 400 μm, density 121 MN/array, (b) length 600 μm, density 361 MN/array, (c) length 600 μm, density 196 MN/array, (d) length 600 μm, density 121 MN/array, (e) length 1000 μm, density 121 MN/array. (f) Photoimage of NC DMN array (630 IU of NC/array, length 600 μm, density 121 MN/array).
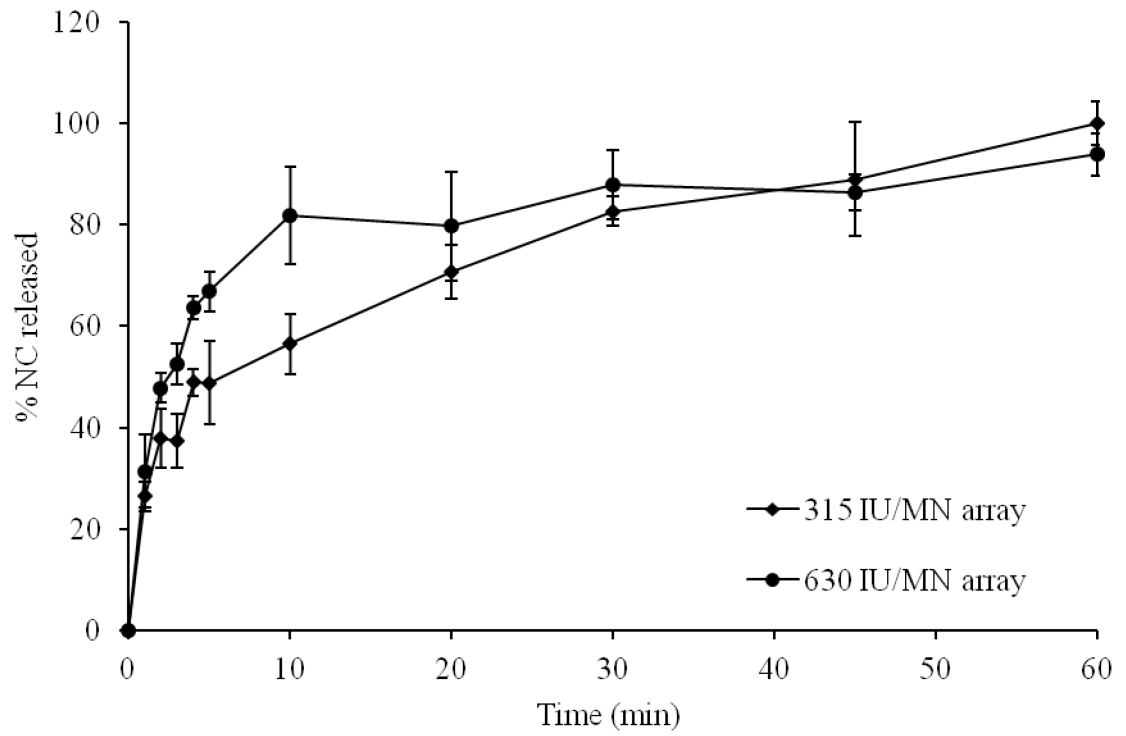
Figure 2. Influence of NC MN loading on NC *in vitro* release in PBS, pH 7.4 at 37°C at fixed needle length of 600 μm and density of 121 MN/array.
Error bars represent SD values; with n ≥ 3.
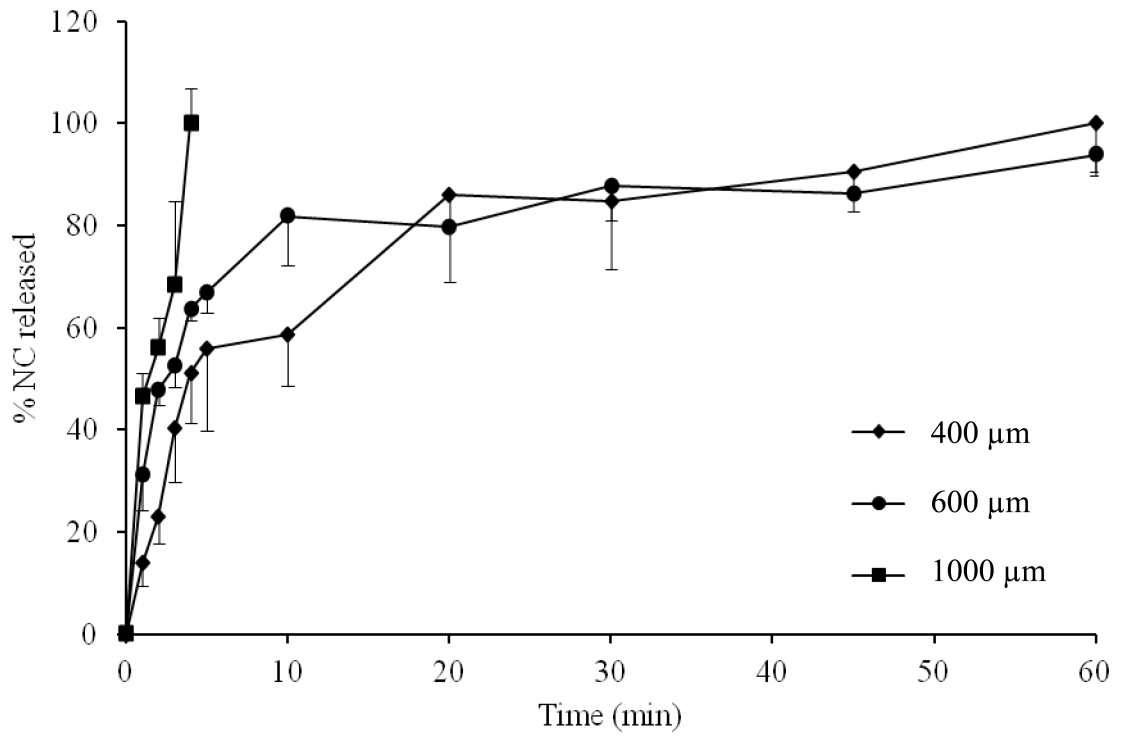
Figure 3. Influence of MN length on NC *in vitro* release in PBS, pH 7.4 at 37°C at fixed NC loading of 630 IU/array and density of 121 MN/array.
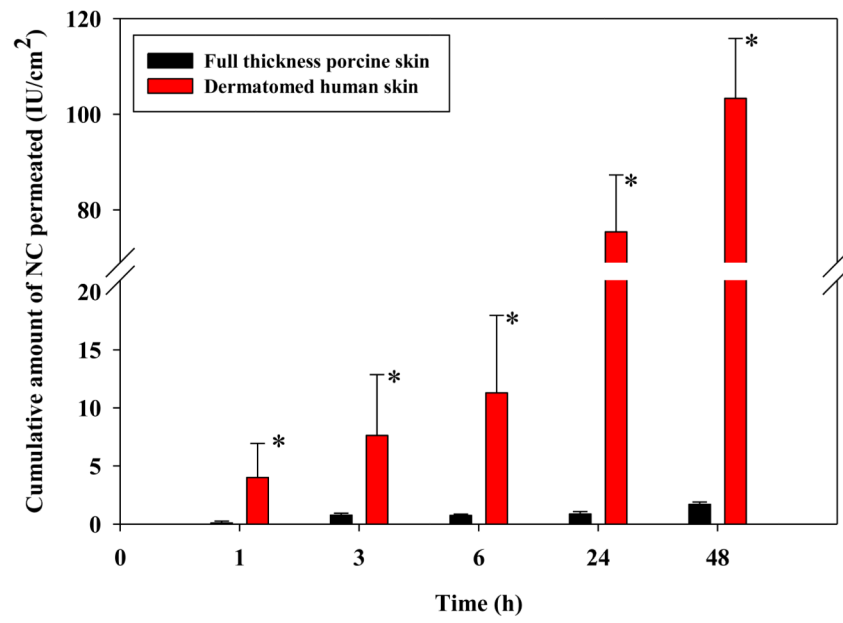Error bars represent SD values; with n   3.
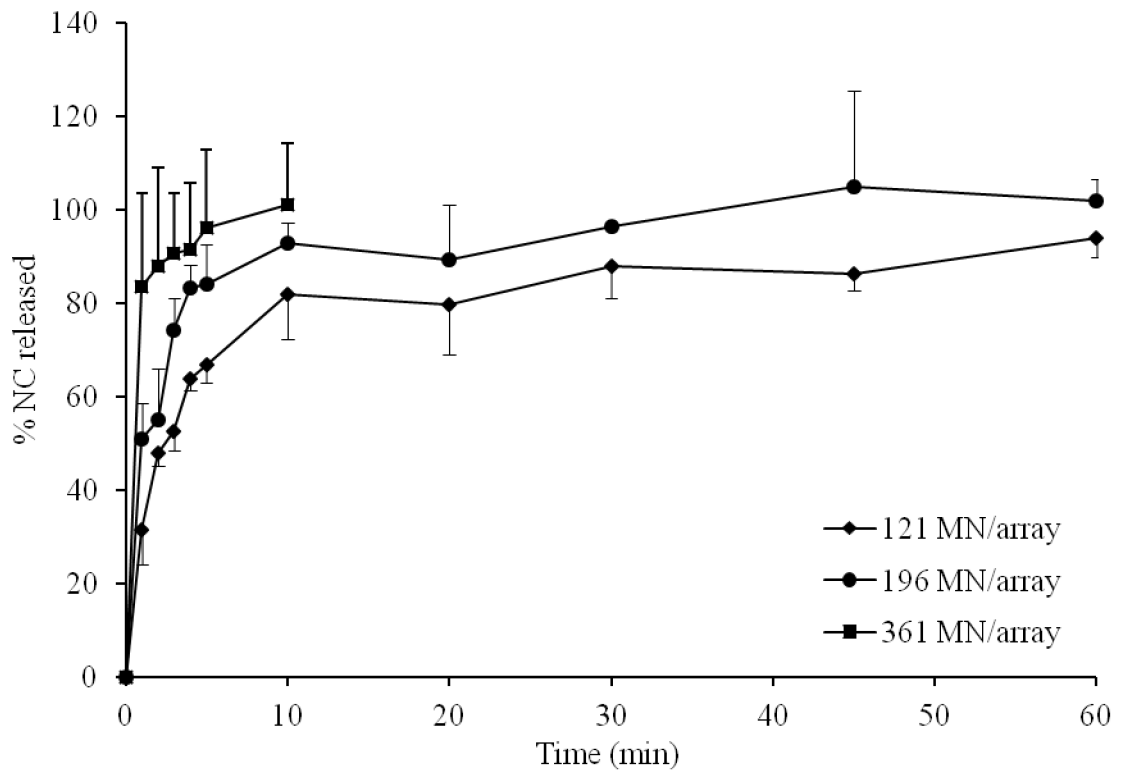
Figure 4. Influence of MN density on NC *in vitro* release in PBS, pH 7.4 at 37°C at fixed NC loading of 630 IU/array and length of 600 μm.
Error bars represent SD values; with n   3.

Figure 5. Influence of skin model on the *in vitro* permeation of NC loaded in DMN arrays (630 IU NC/array, 600 μm long and 121 MN/array dense) at 37°C.
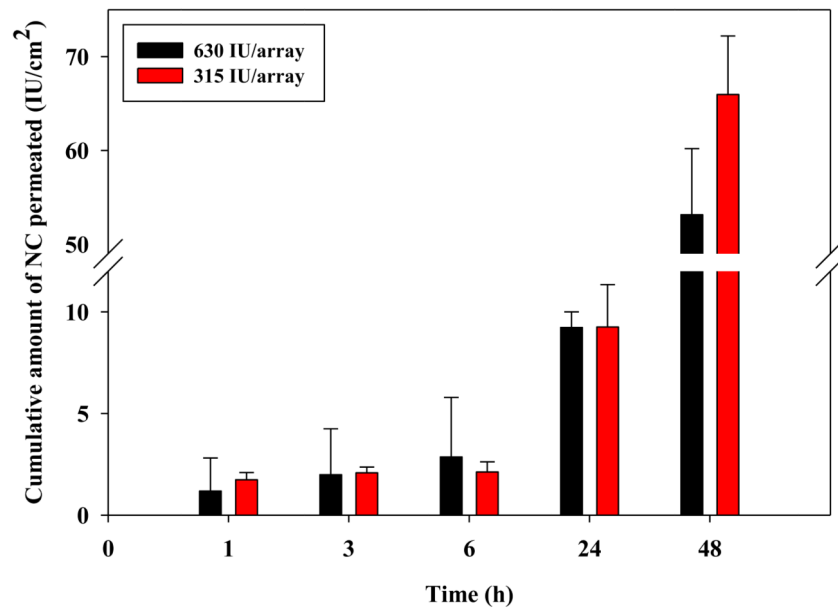Error bars represent SD values; with n 3. *: *P* < 0.005.

Figure 6. Influence of NC loading in DMN arrays (600 μm long and 121 MN/array dense) on its *in vitro* permeation through DHS at 37°C.
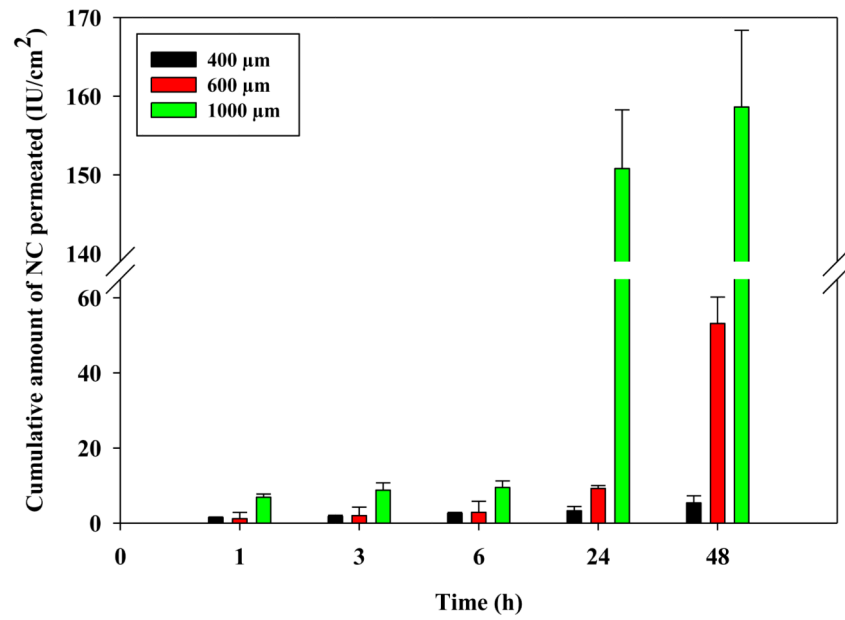Error bars represent SD values; with n 3.

Figure 7. Influence of MN length on the *in vitro* permeation of NC loaded in DMN arrays (630 IU NC/array and 121 MN/array dense) through DHS at 37°C.
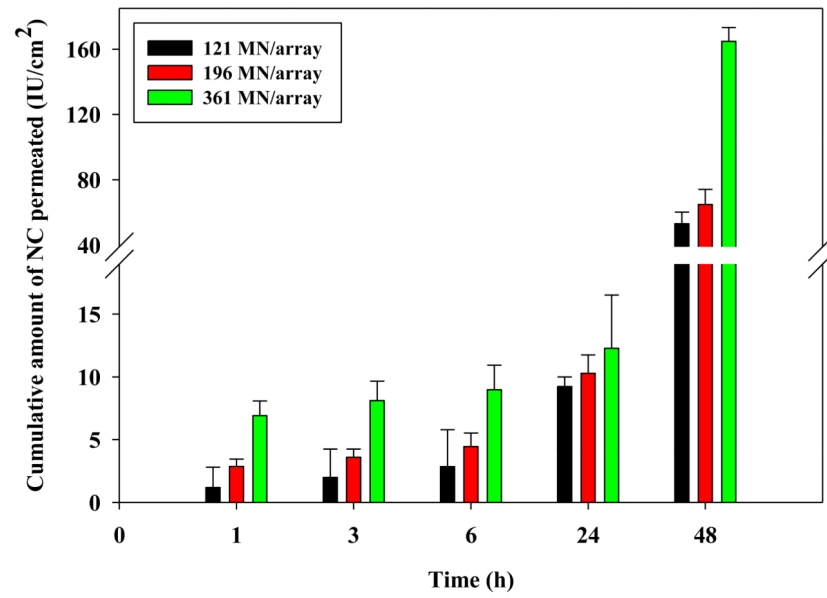Error bars represent SD values; with n = 3.

Figure 8. Influence of MN density on the *in vitro* permeation of NC loaded in DMN arrays (630 IU NC/array and 600 μm long) through DHS at 37°C.
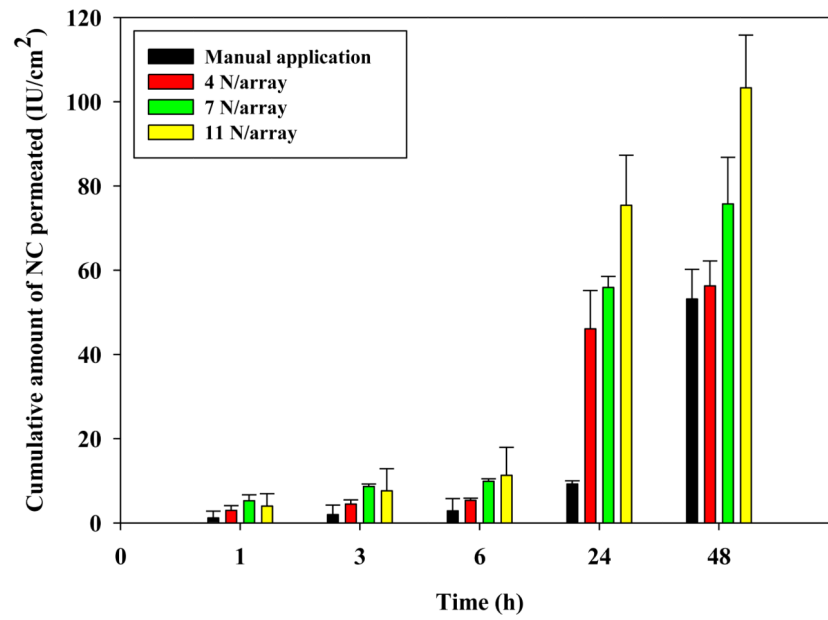Error bars represent SD values; with n 3.

Figure 9. Influence of MN application force on the *in vitro* permeation of NC loaded in DMN arrays (630 IU NC/array, 600 μm long and 121 MN/array dense) through DHS at 37°C.
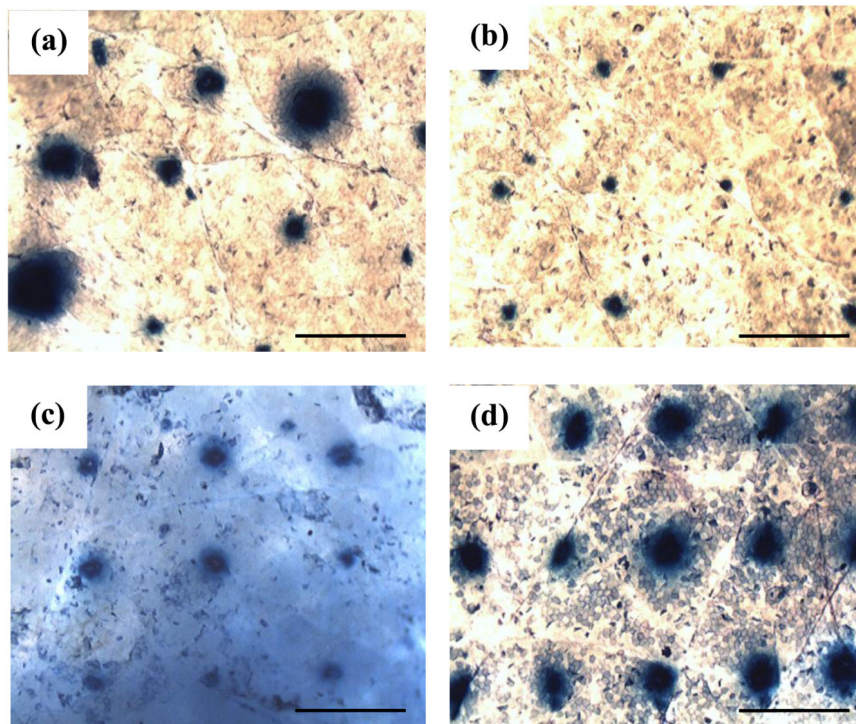Error bars represent SD values; with n 3.

Figure 10. Microscopic images of NC DMN-treated DHS showing the effect of application mode as visualized by trypan blue staining, (a) manual application, (b) applicator at 4 N/MN array, (c) 7 N/MN array, (d) 11 N/MN array.
Bar scales represent 500 μm.

Table 1

Specifications of fabricated NC DMN arrays.

NC loading		Length (μm)	Density (MN/array)
(IU/array)	(% w/w)		
315	1	600	121
630		600	121
945		600	121
630	2	400	121
630	2	1000	121
630	2	600	196
630	2	600	361

Table 2

Specifications of springs used to provide different output forces when inserted in the applicator shaft.

Spring	Wire diameter (mm)	Outside diameter (mm)	Free length (mm)	Number of coils	Output force (N)
A	1.27	21.46	50.8	6.4	4
B	1.27	21.46	63.5	7.5	7
C	1.27	21.46	76.2	9.6	11